Conference proceeding of X-ray and radio emission from young stars

X-ray Variability during Optical Eclipses of a Young Binary System

Kenji Hamaguchi[1,2], Michael F. Corcoran[1,3], Nicholas E. White[1], Ralph Neuhäuser[4], Beate Stelzer[5], Luis A. Balona[6]

[1]*Laboratory for High Energy Astrophysics, Goddard Space Flight Center, Greenbelt, MD 20771, USA*

kenji@milkyway.gsfc.nasa.gov

[2]*National Research Council, 500 Fifth Street, NW, Washington, DC 20001, USA*

[3]*Universities Space Research Association, 7501 Forbes Blvd, Ste 206, Seabrook, MD 20706, USA*

[4]*Astrophysikalisches Institut, Universitaet Jena, Schillergaesschen 2-3, D-07745 Jena, Germany*

[5]*INAF, Osservatorio Astronomico di Palermo, Piazza del Parlamento 1, I-90134 Palermo, Italy*

[6]*South African Astronomical Observatory, PO Box 9, Observatory 7935, Cape Town, South Africa*

ABSTRACT

We report on the *XMM-Newton* observations of the eclipsing binary system TY CrA, performed during the primary eclipse on 2003 March 28 for about 36 ks and the following secondary eclipse on 2003 March 29 for about 32 ks. The observations were intended to search for X-ray eclipses to identify the X-ray emitter, but we detected no X-ray eclipse in these optical eclipses. Instead, we detect a flux increase during the primary eclipse, which does not look like conventional solar-type X-ray flares and seems to coincide with the optical eclipse, while we detect no X-ray variation specific at the secondary eclipse. Surprisingly, between these two eclipses, the plasma temperature in the hot component and X-ray luminosity significantly dropped from 3.3 keV to 1.5 keV and from 1.6×10^{31} ergs s^{-1} to 6×10^{30} ergs s^{-1}, respectively. Whereas the absorption column density ($N_{\rm H}$) did not vary ($\sim4.5\times10^{21}$ cm^{-2}). We discuss the origin of the X-ray emission combining results of earlier observations with *ASCA*, *Chandra* and *XMM-Newton*.

Subject headings: stars: individual (TY CrA)—stars: activity—binaries: eclipsing—stars: pre–main-sequence—X-rays: stars

1. Introduction

The *ASCA* and *ROSAT* satellites have detected X-ray emission from intermediate-mass ($\sim$3–8$M_\odot$) pre-main-sequence (PMS) stars, the Herbig Ae/Be stars (HAeBes) (Zinnecker & Preibisch 1994; Skinner & Yamauchi 1996; Yamauchi et al. 1998; Hamaguchi et al. 2000; Hamaguchi 2001). The X-ray luminosity reaches 10^{32} ergs s^{-1} with plasma temperatures around 2 keV. However, according to the HAeBes evolutionary scenario (e.g. Palla & Stahler 1993), there are no known mechanisms to produce X-ray emission from these stars: neither surface convection to drive a magnetic dynamo as in low-mass stars nor strong UV fields to accelerate unstable stellar winds as in high-mass main-sequence (MS) stars. Hamaguchi (2001) proposes an alternative magnetic dynamo working on HAeBes, which couples the star with its accretion disk, but,

because young low-mass stars tend to be active in X-rays and are usually present around HAeBes (Testi et al. 1998), hidden active low-mass companions might actually produce the observed emission from X-ray bright HAeBes.

If the separation between a HAeBe and its hidden companion is a half-arcsecond or less, even high resolution imaging with *Chandra* would not be able to spatially reveal the X-ray bright companion. One way to confirm that X-ray emission is produced by the HAeBe star itself is to observe an eclipsing HAeBe binary and to look for X-ray time variability correlated with the optical eclipse. Currently, only two eclipsing HAeBes binaries are known: TY CrA (Kardopolov et al. 1981) and MWC1080 (Grankin et al. 1992). However, only the orbital epoch of TY CrA has been intensively studied (Casey et al. 1995, 1998), so that at present, TY CrA is the only target suited for this purpose.

TY CrA is a B7-9 star in the R Coronae Australis (R CrA) star forming region (d ∼130 pc, Marraco & Rydgren 1981; Perryman et al. 1997). TY CrA is an eclipsing binary system with a period of 2.888777 days (Kardopolov et al. 1981). The primary star has $M_1 = 3.2\ M_\odot$, $R_1 = 1.8\ R_\odot$ and $L_1 = 67\ L_\odot$ and the secondary star has $M_2 = 1.6\ M_\odot$, $R_2 = 2.1\ R_\odot$ and $L_2 = 2.4\ L_\odot$ (Casey et al. 1998). Both stars are consistent with the age of 3 Myr. The orbit is almost circular (e <0.007), the orbital semi-major axes are $a_1 = 3.4{\times}10^{11}$ cm and $a_2 = 6.6{\times}10^{11}$ cm, and the inclination of the orbital plane is ∼83° (Casey et al. 1995), and therefore each star is covered by ∼30% during its eclipse. The system also contains a third star having a mass of 1.2–1.5 $M_\odot$ at a separation of 0.9–1.5 AU (Casey et al. 1995; Corporon et al. 1996), whose orbital eccentricity $e \sim 0.3$–0.5 with inclination $i = 70 - 90°$ with respect to that of the binary. In addition, Chauvin et al. (2003) found a stellar object at ∼0.″3 apart from TY CrA, which might be a subsolar mass fourth companion (spectral type ∼M4).

TY CrA was observed three times with *ASCA* SIS CCD camera in observations of the R CrA low-mass protostar cluster (Koyama et al. 1996; Hamaguchi 2001, see table 1). The X-ray emission was constant through these observations (kT ∼1.5 keV, log $L_{\rm X}$ ∼30.5 ergs s^{-1}). These observations included one primary and one secondary eclipses, which means that *ASCA* detected no X-ray time variation specific at the eclipses, suggesting that the emission does not originate with the HAeBe binary. However, the *ASCA* observations have a few weak points: X-ray contamination of the nearby Herbig Be star HD 176386, limited effective area and dead time of ∼50% of total observation time due to earth occultation and passage of high cosmic particle region. Because of these limitations we have re-observed this system with *XMM-Newton* at selected eclipsing phases.

2. Observations

The *XMM-Newton* observation during the primary eclipse (hereafter Obs$_{\rm pr}$) was performed on 2003 March 28 for about 36 ks, which corresponds to the orbital epoch 1104 defined in the ephemeris by Casey et al. (1998) (section 5.1). The observation during the following secondary eclipse (hereafter Obs$_{\rm sec}$) was performed a day after on 2003 March 29 for about 32 ks. The eclipse minima in both observations (orbital epoch 1104.0 and 1104.5) were set to occur in the middle of the observations. All X-ray CCD camera arrays (EPIC MOS and pn) were operated in full frame mode with the medium filter. The grating instrument (RGS) was operated in normal mode. The optical monitor (OM) was blocked due to an optically bright star in the field of view (*fov*). In both observations TY CrA was placed on the prime EPIC position. The satellite position angle was set at 98° so that all X-ray sources detected by *Chandra* (observed on October 10, 2000, hereafter Obs$_{\rm cxo}$) were off the RGS dispersion axis. The analysis was performed with SAS 5.4.1

Table 1: X-ray Observations of TY CrA

Date ⟨yy/mm/dd⟩	Orbital Epoch	Observatory	$kT_{\rm hot}$ ⟨keV⟩	log $L_{\rm X}$ ⟨ergs s^{-1} ⟩	State
94/04/04	0.45–0.81	*ASCA*	1.8	30.4	LS
96/10/18	0.67–0.80	*ASCA*	1.8	30.5	LS
98/10/19	0.87–1.30	*ASCA*	1.2	30.6	LS
00/10/07	0.82–0.90	*Chandra*	2.0 (3.5)	30.7 (31.1)	LS (Flare)
01/04/09	0.38–0.49	*XMM-Newton*	4.5	31.4	HS
03/03/28	0.93–1.08	*XMM-Newton*	3.3	31.2	HS
03/03/29	0.43–0.56	*XMM-Newton*	1.5	30.8	LS

Note — *ASCA* results, which assumes an absorbed 1T model, are referred to Hamaguchi (2001). Numbers in parenthesis show values during the flare maximum. LS: low state, HS: high state.

and LHEASOFT ver. 5.2. To apply the latest calibration data, the EPIC events data were reprocessed from ODF files with the "emchain" and "epchain" SAS scripts.

In advance of the *XMM-Newton* observations, UBVRI photometry of the primary eclipse (2003 March 13) and the secondary eclipse (2003 March 16) was obtained at South African Astronomical Observatory. HD 176423 and HD 176497 were used as comparison stars. The primary eclipse was clearly seen in every band though the recovery was not observed. The light curves were largely consistent with the ephemeris measured by Casey et al. (1998). The secondary eclipse was not recognized.

3. Results

Figure 1 shows a true color image of the EPIC pn *fov* in Obs$_{\rm pr}$, excluding high background intervals (>1cnts s^{-1} above 10 keV in the entire pn chip). The image is color-coded to represent hard X-ray band (2–9 keV) in blue, medium band (1–2 keV) in green and soft band (0.2–1 keV) in red. Embedded or hot sources are shown blue, and cool or unabsorbed sources red. TY CrA is the brightest source at the center in white. Another bright source in the south is the weak-lined T Tauri star CrA 1. Blue weak sources between them are a cluster of low-mass protostar candidates (see Koyama et al. 1996).

Source events were extracted from a 36″ radius circle centered at TY CrA, to include ∼85% of the total photon events. There are two X-ray sources in the vicinity of TY CrA, the Herbig Be star HD 176386 at ∼1′ south and a weak X-ray source at ∼50″ north, which do not severely contaminate the source region. We determined backgrounds from surrounding source free regions: an annulus with 2′ outer radius and 1′ inner radius without any X-ray sources for the MOS observations, and a circle on about the same CCD y column in the same CCD chip (No. 1) as the chip position of TY CrA for the pn. To see X-ray time variability through the observations, we used all the data including high background intervals. Intrinsic background is significant above 4 keV in Obs$_{\rm sec}$ (see the next paragraph). To obtain the best signal-to-noise ratio, background subtracted light curves were made in the 0.5–8 keV band for Obs$_{\rm pr}$ and the 0.5–4 keV band for Obs$_{\rm sec}$ (top panels in figure 2). During high background intervals, the background events were up to 25% of the total counts in Obs$_{\rm pr}$ (for ∼2 ksec at ∼15 ksec, and for ∼7 ksec at the end of the observation) and up to 40% in Obs$_{\rm sec}$ (for ∼20 ksec at ∼15 ksec), while the background levels in low background intervals

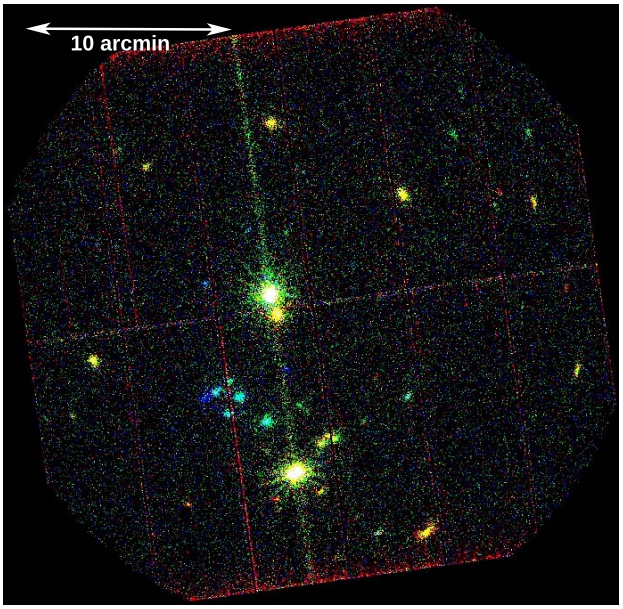

Fig. 1.— A true color image of the R CrA star forming region taken with EPIC pn in $\mathrm{Obs_{pr}}$. Blue, green and red colors represent X-ray emission in 2–9 keV, 1–2 keV and 0.2–1 keV bands, respectively. The white arrow in the top left shows 10′. The north is up and the east is left.

are only ∼2%. Spike due to background in any of the high background intervals was well subtracted in either light curve. In $\mathrm{Obs_{pr}}$, the flux gradually increased from 1.0 cnts $\mathrm{s^{-1}}$ to 1.5 cnts $\mathrm{s^{-1}}$ in 10 ks, and reached maximum when near time of the optical minimum. The flux then gradually decreased with about the same slope as the increase. In $\mathrm{Obs_{sec}}$, the X-ray flux linearly decreased by ∼20%, without no apparent phase-locked variation.

The time-averaged EPIC spectrum in $\mathrm{Obs_{pr}}$ (left panel in figure 3) shows ionized Fe Kα line emission at around 6.7 keV and Ne line at around 1 keV, which is confirmed by the RGS spectra. The continuum emission requires at least two temperature plasmas with kT_{hot} ∼3.3 keV and kT_{cool} ∼0.9 keV (table 2) using the MeKaL code (Mewe et al. 1985, 1986; Kaastra 1992; Liedahl et al. 1995) with common absorption. The metal abundance is small (∼0.2 solar) although the model does not reproduce the structure around 1 keV. The absorption corrected X-ray luminosity is $\sim 1.6\times10^{31}$ ergs $\mathrm{s^{-1}}$. The spectrum in $\mathrm{Obs_{sec}}$ (right panel in figure 3) also requires two temperature plasmas with common absorption. kT_{cool} (∼0.7 keV) is around as same as that in $\mathrm{Obs_{pr}}$, but kT_{hot} is lower, ∼1.5 keV. The X-ray luminosity dropped to $\sim 6\times10^{30}$ ergs $\mathrm{s^{-1}}$. We see a few weak lines between 1–4 keV, which are probably from Si and S. The metal abundance is typical of stellar X-ray emission (∼0.3 solar, e.g. Kitamoto & Mukai 1996). kT_{hot} and L_{X} dramatically dropped over a timescale of a day between $\mathrm{Obs_{pr}}$ and $\mathrm{Obs_{sec}}$. N_{H} (4.6×10^{21} $\mathrm{cm^{-2}}$) did not vary, which suggests that the variation between $\mathrm{Obs_{pr}}$ and $\mathrm{Obs_{sec}}$ is not caused by contamination of an unknown background source, such as an AGN.

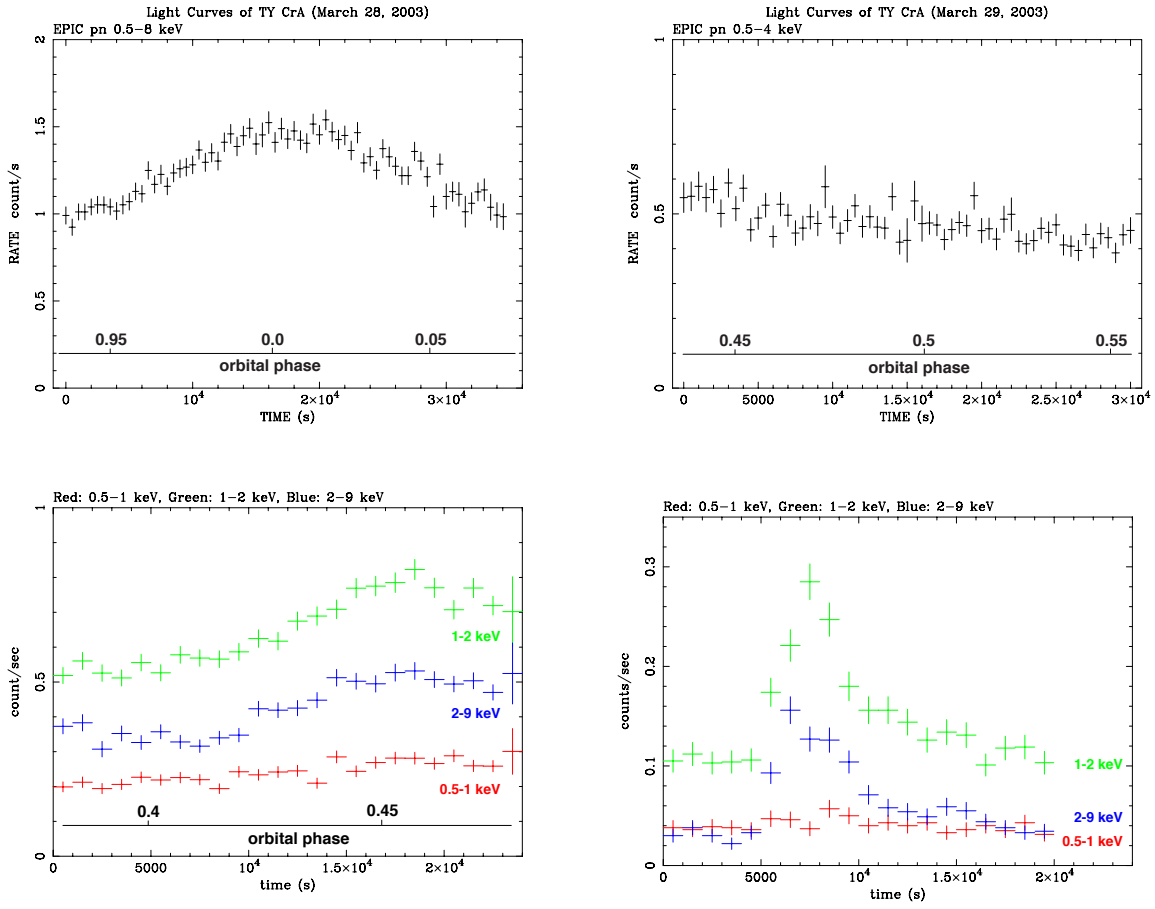

Fig. 2.— Light curves in $\mathrm{Obs_{pr}}$ (top left: 0.5–8 keV), $\mathrm{Obs_{sec}}$ (top right: 0.5–4 keV), $\mathrm{Obs_{2001}}$ (bottom left: multi-band), and $\mathrm{Obs_{cxo}}$ (bottom right: multi-band). See figure 1 of Casey et al. (1998) for optical light curves during the eclipse.

4. Where Does the X-ray Emission Come From?

According to the orbital parameters measured by Casey et al. (1995, 1998), around 30% of the stellar optical disk is covered during the eclipse minimum. Because rotational axes of both stars are generally considered to be perpendicular to the orbital plane, high latitude and polar cap regions should be covered during the primary and secondary eclipses. In the *XMM-Newton* observations, we saw no decrease of X-ray flux during the eclipses. This means that X-ray emission does not mainly come from those regions although emission from the anti-polar region could still be possible. X-ray emission can decrease less than 30% if the X-ray emitting region is much larger than the stellar size, such as a corona. However, the radius of a spherical corona should be $\gtrsim$1.5 R_* not to see significant flux decrease during the observations. The third or fourth companions could be the source of some or all of the X-ray emission though the (non-flaring) X-ray luminosity of 6–20$\times10^{30}$ ergs s^{-1} is too large for most low-mass stars (e.g. Neuhäuser et al. 1995).

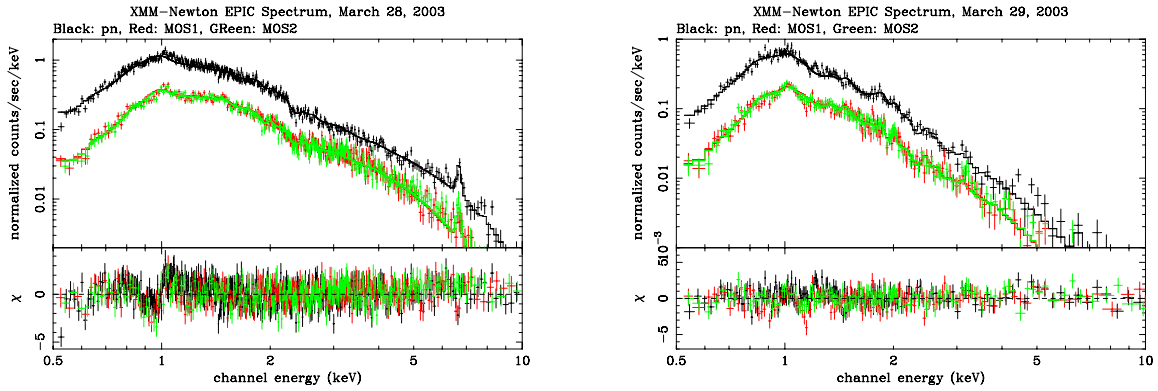

Fig. 3.— X-ray spectra in $\mathrm{Obs_{pr}}$ (left) and $\mathrm{Obs_{sec}}$ (right). Black, red and green show spectra of EPIC pn, MOS1 and MOS2, respectively. Solid lines show the best-fit models by a two temperature models with common absorption.

A big puzzle is the flux increase seen in $\mathrm{Obs_{pr}}$. The phenomenon was completely opposite to our expectation as the star was actually covered. A possible interpretation is that an active hot spot on the primary or secondary surface appears from back of the star by stellar revolution, rotates 180° and disappears to the back again. Casey et al. (1998) suggest that the secondary star has synchronous rotation with the binary revolution while the primary star has sub-synchronous rotation. Then, rotation angles during $\mathrm{Obs_{pr}}$ (∼37 ks) were around 50° for the secondary and less for the primary, which was much less than 180°, and hence, the rotational modulation of a hot spot would not explain the flux variation. The variation may be explained by short time-scale activity of an X-ray emitting hot spot. However, the flux increase does not look like typical flares on low-mass stars, in which X-ray flux rises abruptly in $\lesssim$1 ks and exponentially decays for a long time (1–50 ks). Actually, TY CrA has shown a typical X-ray flare in $\mathrm{Obs_{cxo}}$ (bottom right panel of figure 2).[1] On the other hand, a sun spot has long time-scale activity (∼10 days) (Shibata 1996). If TY CrA has a similar activity, the time-scale can be shorter due to faster rotation (∼26 days for the sun, 3–10 days for TY CrA). However, activity of a sun spot accompanies multiple X-ray flares (see figure 2 of Shibata 1996), while the light curves in $\mathrm{Obs_{pr}}$ showed no apparent X-ray flares. The flux increase does not seem to be explained by an active hot spot.

Light curves in $\mathrm{Obs_{sec}}$ did not show a flux increase, while a similar flux increase was seen in another *XMM-Newton* observation on 2001 April 4, performed just before secondary eclipse (hereafter $\mathrm{Obs_{2001}}$, see bottom left panel of figure 2).[2] The X-ray maximum came ∼5 ks before the optical secondary eclipse minimum so that it is arguable as to whether its X-ray flux increase correlates with the optical eclipse. However, its time scale and shape look like those in $\mathrm{Obs_{pr}}$. Both variations could be the same phenomena which probably would not be like stellar flares because few stellar flares have similar rising time-scale and

[1]Details can be seen in the poster proceeding (IAU2003, S221) by Hamaguchi K. & Corcoran M. F., which can be obtained at ⟨http://www.phys.unsw.edu.au/iau221/poster_pres.htm⟩.

[2]Details can be seen in the same poster proceeding as of the *Chandra* result of TY CrA (IAU2003, S221).

Table 2: Spectral Parameters Fit by an Absorbed 2T Model

		Obs_{pr}	Obs_{sec}
Cool component			
kT	[keV]	0.85 (0.84–0.87)	0.68 (0.66–0.70)
Flux	[ergs cm^{-2} s^{-1}]	8.7e-13	4.0e-13
Hot component			
kT	[keV]	3.3 (3.1–3.5)	1.5 (1.47–1.58)
Flux	[ergs cm^{-2} s^{-1}]	3.8e-12	8.2e-13
Abundance	[solar]	0.18 (0.13–0.22)	0.28 (0.24–0.32)
$N_{\rm H}$	[10^{21} cm^{-2}]	4.3 (4.2–4.5)	4.6 (4.3–4.9)
$L_{\rm X}$	[ergs s^{-1}]	1.6e31	5.8e30
$\Delta\chi^2$ (d.o.f.)		1.26 (916)	1.15 (458)

Note — Number in parentheses shows 90% confidence errors.

amplitude (e.g. Imanishi et al. 2003). Another thing they have in common is $kT_{\rm hot}$ and $L_{\rm X}$, which are large ($kT_{\rm hot}$ ∼4 keV, log $L_{\rm X}$ ∼31.3 ergs s^{-1}, hereafter high state (HS)), compared with $kT_{\rm hot}$ during the other observations including earlier *ASCA* observations ($kT_{\rm hot}$ ∼1.5 keV and log $L_{\rm X}$ ∼30.6 ergs s^{-1}, which we call low state (LS)) (table 1). We investigate the dependence of $L_{\rm X}$ on orbital phase (figure 4). Then, an orbital phase can have both large and small $L_{\rm X}$, i.e. HS and LS. This suggests that HS happens irrespective of the orbital phase.

If the X-ray emission in the HS always increases during eclipses, it should be stronger to the direction parallel to the axis on the primary and secondary stars. A possible interpretation is that absorbing matter within or around the binary system opens to that direction though significant variation of $N_{\rm H}$ required for the flux variation was not observed. Another possibility is that X-rays emit preferably to that direction when they are produced. The only mechanism we can imagine is the inverse Compton process in which stellar UV excites to the X-ray energy by high energy electrons (γ ∼20) streaming parallel to the axis on the primary and secondary stars. In fact, continuum emission in Obs_{2001} and Obs_{pr} can be reproduced with power-law and cool 1T model with common absorption as well, but we have to invoke the 6.7 keV Fe emission line to a hidden hot thin-thermal component.

We appreciate Prof. Shibata K. for useful comments about solar X-ray activity. We should also appreciate the Germany-Japan collaboration program (Inoue, H. and Truemper, J.), by whose support these observations were made possible.

REFERENCES

Casey, B. W., Mathieu, R. D., Suntzeff, N. B., & Walter, F. M. 1995, AJ, 109, 2156

Casey, B. W., Mathieu, R. D., Vaz, L. P. R., Andersen, J., & Suntzeff, N. B. 1998, AJ, 115, 1617

Chauvin, G., Lagrange, A.-M., Beust, H., Fusco, T., Mouillet, D., Lacombe, F., Pujet, P., Rousset, G., Gendron, E., Conan, J.-M., Bauduin, D., Rouan, D., Brandner, W., Lenzen, R., Hubin, N., & Hartung, M. 2003, A&A, 406, L51

Corporon, P., Lagrange, A. M., & Beust, H. 1996, A&A, 310, 228

Grankin, K. N., Shevchenko, V. S., Chernyshev, A. V., Ibragimov, M. A., Kondratiev, W. B., Melnikov, S. Y., Yakubov, S. D., Melikian, N. D., & Abramian, G. V. 1992, *Informational Bulletin on Variable Stars*, 3747, 1

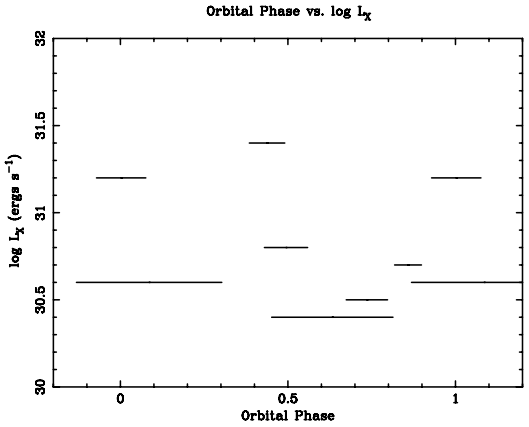

Fig. 4.— Plots of log $L_{\rm X}$ vs. orbital phase. A bar shows X-ray luminosity and orbital phases through its observation.

Hamaguchi, K. 2001, PhD thesis, Kyoto University

Hamaguchi, K., Terada, H., Bamba, A., & Koyama, K. 2000, ApJ, 532, 1111

Imanishi, K., Nakajima, H., Tsujimoto, M., Koyama, K., & Tsuboi, Y. 2003, PASJ, 55, 653

Kaastra, J. S. 1992, "An X-Ray Spectral Code for Optically Thin Plasmas" (Internal SRON-Leiden Report, updated version 2.0)

Kardopolov, V. I., Sahanionok, V. V., & Philipjev, G. K. 1981, *Peremennye Zvezdy*, 21, 589

Kitamoto, S., & Mukai, K. 1996, PASJ, 48, 813

Koyama, K., Hamaguchi, K., Ueno, S., Kobayashi, N., & Feigelson, E. D. 1996, PASJ, 48, L87

Liedahl, D. A., Osterheld, A. L., & Goldstein, W. H. 1995, ApJ, 438, L115

Marraco, H. G., & Rydgren, A. E. 1981, AJ, 86, 62

Mewe, R., Gronenschild, E. H. B. M., & van den Oord, G. H. J. 1985, A&AS, 62, 197

Mewe, R., Lemen, J. R., & van den Oord, G. H. J. 1986, A&AS, 65, 511

Neuhäuser, R., Sterzik, M. F., Torres, G., & Martín, E. L. 1995, A&A, 299, L13

Palla, F., & Stahler, S. W. 1993, ApJ, 418, 414

Perryman, M. A. C., Lindegren, L., Kovalevsky, J., Hoeg, E., Bastian, U., Bernacca, P. L., Crézé, M., Donati, F., Grenon, M., van Leeuwen, F., van der Marel, H., Mignard, F., Murray, C. A., Le Poole, R. S., Schrijver, H., Turon, C., Arenou, F., Froeschlé, M., & Petersen, C. S. 1997, A&A, 323, L49

Shibata, K. 1996, in IAU Colloq. 153: Magnetodynamic Phenomena in the Solar Atmosphere - Prototypes of Stellar Magnetic Activity, 13–+

Skinner, S. L., & Yamauchi, S. 1996, ApJ, 471, 987

Testi, L., Palla, F., & Natta, A. 1998, A&AS, 133, 81

Yamauchi, S., Hamaguchi, K., Koyama, K., & Murakami, H. 1998, PASJ, 50, 465

Zinnecker, H., & Preibisch, T. 1994, A&A, 292, 152

This preprint was prepared with the AAS LaTeX macros v5.0.